Journal of Clinical and Medical Images

ISSN: 2640-9615 / Volume 09

Research article

Open Access

Automated Continuous Measurement of Full-Segment Interventricular Septal Thickness from Long-Axis Echocardiograms via Deep Learning

Xiaoting Zhang, MD, Huizhi Guo, MD, Qin Qin, MD, Chengjin Li, MD and Kai Wu, PhD

Department of Ultrasound, The Third Affiliated Hospital of Shenzhen University (Shenzhen Luohu People's Hospital), No. 47 Youyi Road, Shenzhen 518001, China.

*Corresponding author:
Kai Wu, PhD, Department of Ultrasound, The Third Affiliated Hospital of Shenzhen University (Shenzhen Luohu People's Hospital), No. 47 Youyi Road, Shenzhen 518001, China.

Received Date: 02 Mar 2026
Accepted Date:25 Mar 2026
Published Date: 29 Mar 2026
J Short Name: JCMI

Keywords: Interventricular Septum Thickness; Semantic Segmentation; Deep Learning; Echocardiography; Automated Measurement.

1. Abstract

1.1. Objective

To establish an automated method for measuring interventricular septal (IVS) thickness across its entire length on parasternal long-axis echocardiographic views, providing a continuous and interpretable assessment of myocardial thickness. Methods: A total of 10,319 long-axis view images were retrospectively included. IVS contours were manually delineated and thickness was measured by sonographers. The YOLO deep learning framework was employed for IVS semantic segmentation. The geometric centreline skeleton of the IVS was extracted using a thinning algorithm. Perpendicular distances to this centreline were calculated at 10-pixel intervals to obtain a continuous thickness profile along the IVS long axis. Using manual linear measurements as the gold standard, concordance correlation (PRR), intraclass correlation coefficient (ICC), and mean absolute error (MAE) were computed. Results: The segmentation model achieved a Dice coefficient of 0.85 ± 0.05. Automated thickness measurements showed high agreement with manual results (PRR = 0.92, 95% CI 0.90–0.93; ICC = 0.91, 95% CI 0.90–0.92), with an MAE of only 0.97 mm. Linear regression yielded a slope of 0.95, close to the line of identity. Conclusion: This study achieves highly accurate and fully visualized continuous measurement of IVS thickness across its entire length, overcoming the limitations of the conventional "two-point" measurement approach and offering a novel automated technical pathway.

2. Introduction

Measurement of interventricular septum (IVS) thickness is a crucial indicator for assessing cardiac structure, aiding not only in the early identification of potential cardiovascular diseases but also serving as an evaluation metric for disease severity, risk stratification, and treatment efficacy [1,2]. Echocardiography, due to its convenience and cost-effectiveness, has become the primary imaging modality for evaluating cardiac function parameters like IVS thickness [3]. Currently, conventional IVS thickness measurement requires placing a measurement line perpendicular to the long axis at the level just below the mitral valve tips in the parasternal long-axis view, avoiding the relatively thickened basal segment of the septum [4-6]. This process relies heavily on the manual operation and experiential judgment of sonographers, leading to strong subjectivity, low efficiency, and significant variability.

In recent years, with the advancement of artificial intelligence technologies, deep learning-based methods for assessing cardiac structure and function hold promise for

improving measurement consistency and accuracy [7, 8]. Some studies have used deep learning to predict the locations of key points representing the junctions of the IVS with the ventricular cavities, calculating the distance between these two points as the thickness value [9]. However, septal thickening often exhibits marked regional or heterogeneous patterns, and its anatomical structure in the long-axis view is often curved. Consequently, measurements based on limited key points can only reflect local thickness information of specific myocardial segments, making it difficult to accurately quantify the thickness distribution and variation along the entire length of the IVS.

This study proposes a novel automated method for measuring IVS thickness: First, semantic segmentation of the IVS structure is obtained using a deep learning method; Second, the geometric centreline of the IVS is automatically determined based on the segmentation result; Third, the perpendicular distance in the normal direction is calculated segmentally along this centreline, serving as the thickness measurement for that IVS segment. This study is the first to achieve segment-by-segment, visualized thickness assessment of the IVS on the long-axis view, potentially providing a more comprehensive and interpretable automated measurement tool for clinical practice.

3. Materials and Methods

3.1. Study Population

This study retrospectively enrolled subjects who underwent echocardiographic examination at Shenzhen Luohu People's Hospital between January 2021 and December 2024, totaling 4,605 participants (age 52.6 ± 16.9 years), including 47 diagnosed with dilated cardiomyopathy and 31 with hypertrophic cardiomyopathy. Inclusion criteria: 1) Age over 18 years; 2) Availability of clear parasternal long-axis views. Exclusion criteria: Missing images or unclear visualization of the IVS. This study was approved by the local hospital's ethics committee (No. 2025-LHQRMYY-KYLL-087), and informed consent was waived due to its retrospective nature.

3.2. Data Processing and Image Annotation

Each ultrasound image was annotated by two sonographers (each with over five years of echocardiography diagnostic experience) who manually outlined the outer contour of the IVS using dense points (Labelme v5.8.2 software). The contour points were placed at the border between the myocardium and the ventricular cavity, ensuring that the measurement included only the compact myocardium of the IVS, avoiding incorporation of right ventricular trabeculations, moderator band, or tricuspid valve structures into the IVS thickness. When the contours outlined by the two sonographers differed significantly (Dice coefficient difference >10%), a third ultrasound expert (with over ten years of experience) performed a review (Figure 1).

During image processing, a total of 10,319 parasternal long-axis ultrasound images were included in this study. The images were randomly split by subject into training (8,224 images), validation (1,047 images), and test (1,048 images) sets in an 8:1:1 ratio. For the test set, two sonographers (each with over five years of experience) manually measured the IVS thickness using straight lines (Labelme v5.8.2 software) on a per-image basis, and these measurements were used to calculate the manual IVS thickness values. When the measurements from the two sonographers differed significantly (>10% difference), a third ultrasound expert (with over ten years of experience) performed a review (Figure 1).

3.3. Model Construction of the IVS Segmentation

The semantic segmentation model for the IVS on long-axis view images was built using the lightweight deep learning segmentation framework YOLOv11-Seg [10]. Compared to conventional segmentation models such as U-Net, this framework integrates object detection and semantic segmentation modules, which helps improve the specificity of IVS identification. During training, the IVS contours drawn by the sonographers were converted into binary segmentation masks. The ultrasound images and corresponding masks were randomly augmented with a 1/3 probability of horizontal

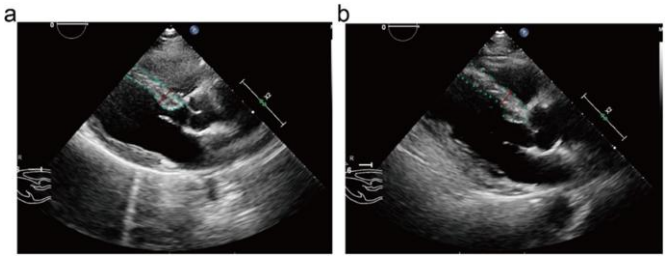

Figure 1: Examples of IVS segmentation and thickness measurement annotation. (a-b) Annotation results by sonographers on two long-axis view echocardiograms: green points outline the IVS contour, red straight lines indicate the location and length for IVS thickness measurement.

flipping, scaling, translation, and adjustments to brightness and contrast (all within ±20%). Images were resized proportionally to a fixed size of 448×448 pixels, and pixel values were normalized to the [0, 1] range. The model utilized a combined loss function consisting of Dice Loss, Cross-Entropy Loss, IoU Loss, and Distribution Focal Loss. Model parameters were optimized using stochastic gradient descent. After 1,000 training epochs, the parameters (including deep learning weights) achieving the highest Dice coefficient on the 1,047-image validation set were selected as the final model.

3.4. Automated Measurement of IVS Thickness

Based on the IVS segmentation results, we designed an automated quantification scheme integrating geometric algorithms for full-segment IVS thickness: 1) Geometric Centerline Skeleton Extraction and Smoothing: The predicted binary IVS segmentation mask was processed using the Zhang-Suen thinning algorithm [11] to obtain a single-pixel-wide geometric centreline skeleton; the entire skeleton coordinates were smoothed using cubic polynomial fitting. 2) Segmented Centreline and Segment-wise perpendiculars: The smoothed centreline was uniformly divided into small segments at 10-pixel (approximately 2 mm) intervals. For the pixel points within each segment, least squares linear fitting was performed to calculate the slope of the perpendicular line for that segment. 3) IVS Thickness Computation per Segment: Using the perpendicular line of each segment as the measurement baseline, the distance between its two intersections with the upper and lower IVS contours was computed, representing the IVS thickness within that minute segment. The thickness values from all segments formed a continuous thickness distribution along the IVS centerline, visually displaying the complete IVS thickness profile on the long-axis view. The proposed automated IVS measurement and analysis pipeline is illustrated in Figure 2.

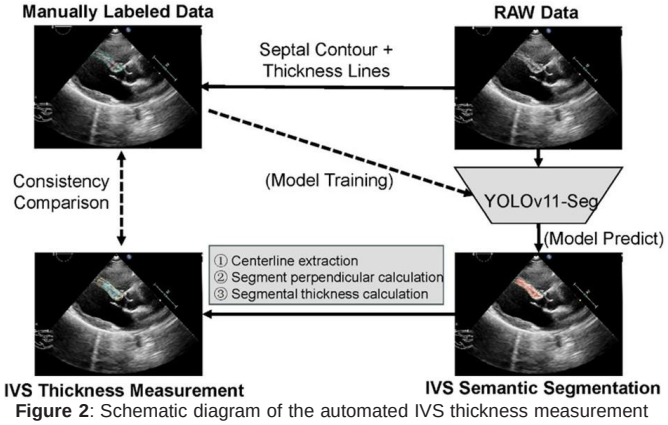

Figure 2: Schematic diagram of the automated IVS thickness measurement workflow. The YOLOv11-Seg model, trained on data annotated by sonographers, directly performs semantic segmentation of the IVS on the original long-axis view images. By extracting the centerline skeleton, generating segmental perpendiculars, and computing thickness segment-by-segment, we achieved fully automated IVS thickness measurement and verified its consistency against manual readings.

4. Statistical Analysis

All deep learning model training and statistical analyses involved in this study were performed using Python (v3.12.4) and R (v3.6.3). Model segmentation performance was evaluated on the test set using the Dice coefficient. Although the automated measurement method outputs multiple segmental thickness values, the median of all segmental thicknesses was taken as the final model measurement value for comparison with manual measurements. Pearson's Correlation Coefficient (PCC) and the Intraclass Correlation Coefficient (ICC) were used to assess the agreement between model and sonographer measurements. A coefficient above 0.75 indicates high agreement. The Mean Absolute Error (MAE) was used to quantify the difference between model and sonographer measurements. All statistical analyses involved two-sided tests, calculating 95% confidence intervals (95% CI), with the statistical significance threshold set at $P = 0.05$.

5. Results

5.1. IVS Semantic Segmentation

The IVS segmentation model, built based on the YOLOv11-Seg framework using 8,224 training images, demonstrated excellent accuracy on the long-axis view. Segmentation results on the test set are shown in Figures 3a–3c: the model accurately outlined the IVS boundaries at end-diastole, mid-diastole, and systole. On the 1,048-image test set, the model achieved an average Dice coefficient of 0.85 ± 0.05 (Figure 3d).

5.3. Automated IVS Thickness Measurement

Leveraging the binary masks produced by IVS segmentation, this study realized fully automated IVS-thickness quantification in the parasternal long-axis view through three sequential steps: centreline skeleton extraction, generation of segment-wise perpendiculars, and segment-specific thickness computation (Figure 2). Figure 4 visualizes the calculation process: the yellow contour represents the model-predicted IVS edges, the red curve is the smoothed geometric centreline skeleton, and the blue line segments are

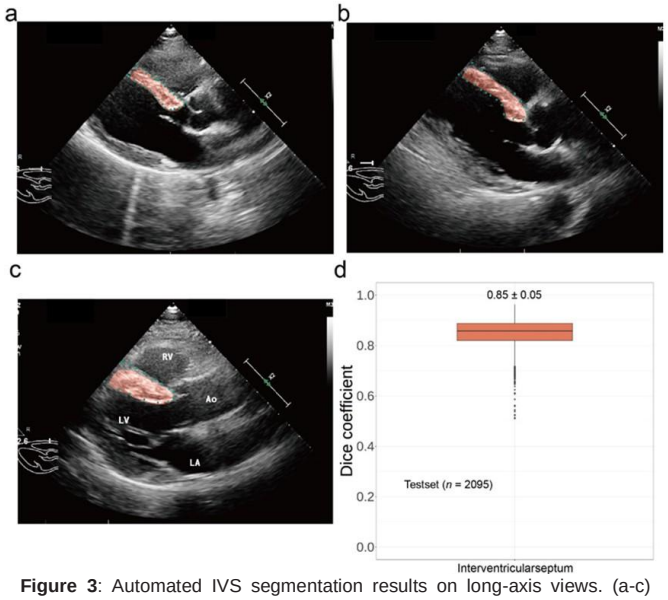

Figure 3: Automated IVS segmentation results on long-axis views. (a-c) Model prediction results for IVS segmentation on long-axis view images from the test set. Red areas represent the model-predicted IVS region; green points indicate the manually annotated IVS contours by sonographers. (d) Statistical performance of the model for IVS segmentation on the test set: the average Dice coefficient for the 1,048 test images was 0.85, with a standard deviation of 0.05.

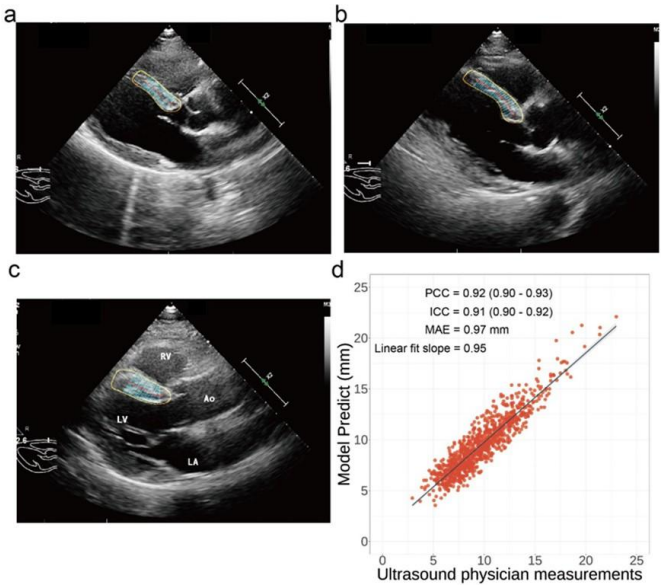

Figure 4: Automated IVS thickness measurement results on long-axis views. (a-c) Examples of continuous segmental thickness measurement in the test set: yellow contour indicates the model-predicted IVS edges; internal red line represents the geometric centerline skeleton of the IVS calculated from the segmentation mask; blue line segments perpendicular to the skeleton are the thickness measurement lines for each segment. (d) Agreement comparison between automated IVS thickness measurements and sonographer measurements.

the thickness measurement lines perpendicular to the skeleton. Figures 4a–4c display the IVS thickness measurement results at end-diastole, mid-diastole, and systole, respectively, showing that the IVS skeleton and its perpendicular lines adapt to changes in IVS curvature and thickness, ensuring measurement is always aligned with the anatomical orientation of the IVS.

In the 1,048-image test set, the manually measured IVS thickness by sonographers was 9.65 ± 2.89 mm; the model output was 9.45±2.77 mm. Statistically, the two measurement results showed high agreement: PCC was 0.92 (95% CI: 0.90–0.93), ICC was 0.91 (95% CI: 0.90–0.92), and the MAE was 0.97 mm. Linear regression fitting yielded a slope of 0.95, close to the line of identity (slope = 1.0) (Figure 4d), indicating high agreement and minimal bias between the model and sonographers in IVS thickness measurement.

6. Discussion

IVS thickness serves not only as an important indicator for assessing cardiac structure and function but also as a diagnostic marker for cardiovascular diseases such as hypertrophic cardiomyopathy [12], coronary artery disease, hypertensive heart disease [13], and cardiac amyloidosis [14], and can be used for risk stratification and treatment evaluation. Changes in its measured value can indicate pathological myocardial alterations. However, traditional echocardiography relies on manual positioning and outlining by physicians, and measurement accuracy depends heavily on operator experience, leading to significant subjective variability. In recent years, with the development of AI technologies, automated measurement methods have been developed and applied to cardiac parameter quantification in imaging.

Existing methods for IVS thickness measurement primarily adopt a "two-key-point" regression strategy: one study integrated 23,745 multi-centre echocardiograms, using deep learning to directly identify the key measurement points on both sides of the IVS in the long-axis view and calculating the Euclidean distance between them as the thickness, reporting an error of 1.2 mm [9].

However, the "two-key-point" strategy overlooks the variability in myocardial morphology distribution and may inadvertently include intracavitary structures like trabeculations or chordae tendineae within the measurement range, potentially leading to significant thickness measurement bias [15]. While semantic segmentation-based methods have been used for cardiac chamber area measurement and function assessment, they are rarely applied to myocardial thickness measurement. Holste et al. [16] developed a large-scale multi-task cardiac function assessment system that used segmentation results for ejection fraction estimation (error 4.5%) and achieved an

accuracy of 0.95 for identifying systolic dysfunction, showing high precision in internal and external validation. Leclerc et al. [17] developed a deep learning model for left ventricle segmentation, achieving a correlation of 0.96 with manually measured areas and an error of 7.6 mL. Ouyang et al. [18] achieved video-level left ventricle segmentation in the apical four-chamber view, tracking LV area changes during cardiac motion, with a segmentation Dice coefficient of 0.92 and an AUC of 0.97 for discriminating impaired ejection fraction.

To our knowledge, this study is the first to establish an automated thickness measurement model based on IVS semantic segmentation on a dataset of over ten thousand long-axis view echocardiograms, achieving automatic contour delineation of the IVS. Compared to previous automated myocardial thickness studies relying on “two key points”, this study, through three automated computational steps-segmentation, skeletonization, and perpendicular line calculation-achieves continuous segmental measurement of IVS thickness. To balance segmentation accuracy and algorithmic efficiency, this study employed the lightweight YOLO framework that integrates object detection and semantic segmentation, capable of outputting highly accurate segmentation masks while maintaining real-time performance. On the 1,048-image test set, the model's overall Dice was 0.85 ± 0.05 (Figure 3d). Although the segmentation Dice did not reach above 0.90, the standard deviation was only 0.05, indicating good stability of the model’s segmentation.

Further analysis revealed that the regions where the Dice was below 0.90 were concentrated in the apical segment (left segment) of the IVS, where boundaries are often indistinct, making precise contour delineation difficult. In contrast, the basal segment (right segment) near the aorta has clear contours and high contrast, where the model's segmentation accuracy was significantly better than in the apical segment (Figures 3a-3c). Since clinical thickness measurements are typically performed at the mid-septal level near the mitral valve, and the skeleton ends fall within non-measurable regions during geometric skeleton extraction via the thinning algorithm (Figures 4a-4c), we believe the impact of segmentation errors in the apical segment on the final thickness measurement is limited. Consequently, the model's measurement results showed high agreement with manual sonographer measurements, with an ICC of 0.91 (95% CI 0.90–0.92), and very low bias, with an MAE of only 0.97 mm (Figure 4d).

The visualization capability of our automated measurement enhances the interpretability of the thickness values. By calculating the perpendicular slope and segment length sequentially along the geometric centerline, the thickness computation consistently adapts to variations in IVS thickness and curvature (Figure 4a-4c). This provides sonographers with an automated quantification tool for segmental myocardial thickening. The thickness measurement method proposed here, based on the output mask from deep learning semantic segmentation, can potentially be applied not only to the long-axis view but also to multi-segment myocardial thickness measurement in apical and short-axis views, demonstrating methodological versatility.

This study has several limitations. The data originated from a single centre, and the types of echocardiographic acquisition equipment were relatively homogeneous. Future work plans include multi-centre validation, incorporating participants with different machine models, age groups, and various cardiovascular diseases for external validation. Furthermore, although the proposed measurement method can adapt to IVS thickness measurement throughout the cardiac cycle, it currently lacks built-in cardiac phase determination, requiring sonographers to determine the phase manually. We plan to incorporate mitral valve motion trajectory analysis as a cardiac phase discrimination indicator in subsequent studies to enhance automation levels and clinical application value.

In conclusion, the automated IVS measurement method proposed in this study combines high visualization and interpretability, overcoming the limitations of the traditional "two-point" measurement approach, and provides a new technical pathway and automated method for myocardial quantitative analysis.

Funding

This study was supported by the National Natural Science Foundation of China (82503972) and Shenzhen Medical Research Fund (C2401015).

References

1. Aimo A, Tomasoni D, Porcari A, Vergaro G, Castiglione V, Passino C: Left ventricular wall thickness and severity of cardiac disease in women and men with transthyretin amyloidosis. European Journal of Heart Failure. 2023; 25(4): 510-514.
2. Luigetti M, Vitali F, Romano A, Sciarrone MA, Guglielmino V. Emerging multisystem biomarkers in hereditary transthyretin amyloidosis: a pilot study. Scientific Reports. 2024; 14(1): 18281.

3. Medicine EGoCSoU, Association ECoCUD: Guidelines for clinical application of echocardiographic assessment of cardiac systolic and diastolic function. Chinese Journal of Ultrasonography. 2020; 29(6): 461-477.
4. Lang RM, Badano LP, Mor-Avi V, Afilalo J, Armstrong A. Recommendations for Cardiac Chamber Quantification by Echocardiography in Adults: An Update from the American Society of Echocardiography and the European Association of Cardiovascular Imaging. Journal of the American Society of Echocardiography. 2015; 28(1): 1-39.
5. Xie M, Jiang Y. Chinese expert consensus for standard assessment by transthoracic echocardiography (2024 edition). Chinese Journal of Ultrasonography. 2024; 33(1): 1-13.
6. Chen M, Lee W-H, Lu C-H, Chang H-C, Tung C-C, Siow Y-Y, Lee H-C. 2025 Expert Consensus Recommendations for the Diagnostic Requirements in Routine Practices of Transthoracic Echocardiography. Acta Cardiol Sin. 2025; 41(1): 1-49.
7. Poterucha TJ, Jing L, Ricart RP, Adjei-Mosi M, Finer J, Hartzel D. Detecting structural heart disease from electrocardiograms using AI. Nature. 2025; 644(8075): 221-230.
8. Yang X-y, Li Y-m, Wang J-y, Jia Y-h, Yi Z, Chen M. Utilizing multimodal artificial intelligence to advance cardiovascular diseases. Precision Clinical Medicine. 2025; 8(3).
9. Duffy G, Cheng PP, Yuan N, He B, Kwan AC, Shun-Shin MJ, Alexander KM. High-Throughput Precision Phenotyping of Left Ventricular Hypertrophy with Cardiovascular Deep Learning. JAMA Cardiology. 2022; 7(4): 386-395.
10. Jocher G, Qiu J. Ultralytics YOLO11. In., 11.0.0 edn. 2024.
11. Zhang TY, Suen CY. A fast parallel algorithm for thinning digital patterns. Commun ACM 1984, 27(3):236–239.
12. Haland TF, Edvardsen T: The role of echocardiography in management of hypertrophic cardiomyopathy. Journal of Echocardiography. 2020; 18(2): 77-85.
13. Levy D, Garrison RJ, Savage DD, Kannel WB, Castelli WP. Prognostic Implications of Echocardiographically Determined Left Ventricular Mass in the Framingham Heart Study. New England Journal of Medicine. 1990; 322(22): 1561-1566.
14. Liang S, Liu Z, Li Q, He W, Huang H. Advance of echocardiography in cardiac amyloidosis. Heart Failure Reviews. 2023; 28(6): 1345-1356.
15. Yukina H, Kusunose K. AI in Echocardiography: State-of-the-art Automated Measurement Techniques and Clinical Applications. Jma j. 2025; 8(1): 141-150.
16. Holste G, Oikonomou EK, Tokodi M, Kovács A. Complete AI-Enabled Echocardiography Interpretation With Multitask Deep Learning. JAMA. 2025.
17. Leclerc S, Smistad E, Østvik A, Cervenansky F, Espinosa F. A Multistage Attention Network to Improve the Robustness of Segmentation of Left Ventricular Structures in 2-D Echocardiography. IEEE Transactions on Ultrasonics, Ferroelectrics, and Frequency Control. 2020; 67(12): 2519-2530.
18. Ouyang D, He B, Ghorbani A, Yuan N, Ebinger J, Langlotz CP. Video-based AI for beat-to-beat assessment of cardiac function. Nature. 2020; 580(7802): 252-256.